Ligand-controlled Synthesis, Reactivity and Oxo-Transfer Kinetics of Oxomolybdenum-(VI) and -(IV) Complexes

Samiran Bhattacharjee and Ramgopal Bhattacharyya*
Department of Chemistry, Jadavpur University, Calcutta 700 032, India

Trifunctional (ONS) dianionic Schiff-base ligands L^{2-} [H_2L = *S*-methyl 3-(2-hydroxyphenyl)methylenedithiocarbazate or 5-R substituent derivatives (R = H, Me, Cl, Br or NO_2) or a naphthyl derivative], in sharp contrast to the *S*-benzyl analogues (H_2L') form only Mo···O→Mo bridged oligomers [$(MoO_2L)_n$] in EtOH or MeOH, irrespective of the substituent R. However, these substituents R control the position of the ν(Mo···O→Mo) vibration, the Mo^{VI}–Mo^{V} redox couple, the ligand-to-metal charge-transfer transition, as well as the chemical shift of the azomethine proton signal and the asymmetric ν(Mo=O) vibration in solution, for both the polymeric complexes and, where relevant, the donor molecule (D) co-ordinated monomers [$MoO_2L(D)$] [D = pyridine (py), dimethylformamide (dmf) or Me_2SO]. Reaction of [MoO_2L] with PPh_3 in CH_2Cl_2, MeOH or MeCN or in donor solvents D (dmf or py) produced oxomolybdenum(IV) derivatives, [MoO(L)] or [MoOL(D)], respectively. The kinetics of oxo transfer from MoO_2^{2+} to PPh_3 occurs in a second-order process. The rate constant of the oxo-transfer reaction from the polymer [$(MoO_2L)_n$] (R = H) to the PPh_3 substrate is $\approx 10^2$ times higher than that of the corresponding monomer [$MoO_2L(D)$]. Both [MoO(L)] and [MoOL(dmf)] react with the Me_2SO substrate in CH_2Cl_2 or dmf in a two-stage process. The first involves the equilibrium formation of a Me_2SO adduct while during the second stage an intramolecular oxo transfer occurs from Me_2SO to the MoO core *via* the elimination of Me_2S. The rate constant of the reverse oxo transfer (k_{-1}) is almost identical for both the polymer [MoO(L)] and monomer [MoOL(dmf)] but the equilibrium constant, *K*, for the formation of the Me_2SO complexed species is slightly higher for [MoOL(dmf)] than for [MoO(L)].

Oxo-transfer chemistry of molybdenum, and, to a lesser extent that of tungsten, ruthenium, osmium and rhenium, is of topical interest.[1] Molybdenum has a special place in this type of chemistry owing to the biological relevance of the model reaction (1)† involving oxo-transfer molybdoenzymes.[2–5] The

$$[Mo^{VI}O_2(\text{ligand})_n] + X \rightleftharpoons [Mo^{IV}O(\text{ligand})_n] + XO \quad (1)$$

oxo-transfer ability of the MoO_2^{2+} core depends on the functionalities present in the ligands. In a number of model studies,[6–9] the indispensibility of at least one sulfur donor was realised.[10] Recently, however, it has been shown that the NNN functionalities generated by a pyrazolylborate ligand[11] also activate the MoO_2^{2+} unit towards oxo transfer. Extended X-ray absorption fine structure (EXAFS) spectroscopic studies have also implicated the presence of a sulfur atom, besides oxygen and nitrogen, at the active sites of oxo-transfer molybdoenzymes.[12–15] We have shown[16] for the ONS-donor dianions of the Schiff-base ligands, *S*-benzyl 3-(5-R-2-hydroxyphenyl)methylenedithiocarbazate, H_2L', that phenyl substituents R (R = H, Me, Cl or Br) play a vital role in controlling whether the isolated dioxomolybdenum(VI) complexes are discrete monomers [$MoO_2L'(D)$] (D = weak donor solvent molecule, *e.g.* EtOH or MeOH) or polymeric species, [$(MoO_2L')_n$], containing ...(O)Mo=O→Mo(O)=O... chains, observed previously[17,18] in [MoO_2(tridentate)] species. The electron-releasing 5-Me substituent yielded a polymer, whilst electron-withdrawing substituents (5-Cl or 5-Br) favoured the formation of monomers.

The present work shows that if the electron-releasing methyl group is substituted for benzyl at the unco-ordinated S atom of H_2L' the new ligands H_2L, shown in thione and thiol form

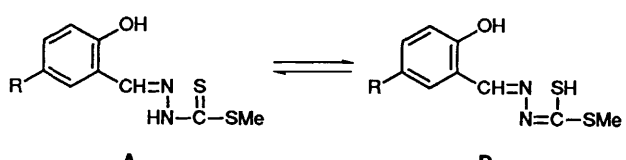

	R
H_2L^1	H
H_2L^2	Me
H_2L^3	Cl
H_2L^4	Br
H_2L^5	NO_2
H_2L^6	5,6-C_4H_4

as **A** and **B**, respectively, afford only polymers, [$(MoO_2L)_n$], even if the 5-R substituent is a strong electron withdrawer such as NO_2. However, for both sets of ligands H_2L' and H_2L it is possible to correlate the Hammett σ_p values of the 5-R substituents with various physico-chemical and spectroscopic parameters of the isolated complexes [MoO_2L] or [MoO_2L']. This correlation study has a practical significance: the remote-control effect of the S- and phenyl-substituents on the structures and chemical and spectroscopic properties of the oxomolybdenum complexes studied here may help to identify the presence of different fragments or substituents attached to the active sites of relevant molybdoenzymes. The present work also shows that the oxo-transfer rate constant from MoO_2 to the substrate is much higher when the oxygen atom is transferred from an oxygen-bridged oligomer, [$(MoO_2L)_n$] than from a discrete monomer, [MoO_2L(dmf)] (dmf = dimethylformamide). A number of reports concerning substituent effects[6a,b,19] and oxo-transfer kinetics[6c,20] in other oxomolybdenum systems, have been published previously.

† Model studies mainly concern tertiary phosphines as the substrate X.

Experimental

Physical Measurements.—Infrared spectra were recorded as KBr discs on a Perkin-Elmer 597 spectrophotometer, and in dmf solution on a Perkin-Elmer 1710 FT-IR spectrophotometer using a demountable Irtran 2 (ZnS) cell, electronic spectra on a Hitachi U-3400 UV/VIS/NIR spectrophotometer, ^{1}H NMR spectra using a Varian EM 390 (90 MHz) spectrometer and $SiMe_4$ as standard. Thermoanalyses were made on a Shimadzu thermoanalyser DT 30. Voltammetric measurements were made with a PAR model 370-4 electrochemistry system: model 174A polarographic analyser, model 175 universal programmer, model RE 0074 XY recorder, model 173 potentiostat, and model 377A cell system. All experiments were performed at 298 K under a dinitrogen atmosphere in a three-electrode configuration using a planar Beckman model 39273 platinum-inlay working electrode, a platinum-wire auxiliary electrode and a saturated calomel reference electrode (SCE). Coulometry was carried out using a 273 potentiostat/galvanostat with a 377 cell system equipped with a platinum-wire-gauze working electrode. The potentials reported are uncorrected for the junction contribution. Magnetic susceptibilities were obtained by the Gouy method using $Hg[Co(NCS)_4]$ as the calibrant. Solution conductances were measured with a Systronics (India) model 304 digital conductivity meter. A Knauer (Berlin) vapour-pressure osmometer was used for the molecular weight determination, calibrated with benzyl solution in an appropriate solvent. Elemental analyses were performed using a Perkin-Elmer 240C elemental analyser and molybdenum was estimated by a gravimetric method.[21] The kinetic measurements were performed under a dinitrogen atmosphere employing 2×10^{-4} mol dm^{-3} dmf–CH_2Cl_2 solutions of the dioxomolybdenum(VI) and oxomolybdenum(IV) complexes. Pseudo-first-order conditions were maintained throughout by use of an excess of PPh_3 over the molybdenum concentration. The time dependence of the absorbance at 464 nm (for complexes of H_2L^1 and H_2L^2) and 462 nm (for complexes of H_2L^3 and H_2L^4) were recorded on a Philips Analytical SP8-150 UV/VIS spectrophotometer with a thermostatted (HAAKE F3) cell compartment. The observed rate constants were obtained from plots of $\ln(A_\infty - A_t)$ or $\ln(A_t - A_\infty)$ *vs.* time, where A_t and A_∞ are the absorbances at time t and infinity, respectively. These were all linear up to four half-lives of the reaction. Data were extracted using a least-squares computer-fitting program.

Materials.—Ammonium heptamolybdate (J. T. Baker, Phillipsburg, NJ), *p*-chlorophenol (AR BDH, UK) and *p*-cresol (S. D. Chemicals, India) were obtained commercially and used as such. The complexes $[MoO_2(acac)_2]$ (acac = acetylacetonate),[17] [MoOL'] (L' = L$^{1'}$–L$^{4'}$),* *S*-methyldithiocarbazate[22] and 5-nitrosalicylaldehyde[23] were prepared by the literature methods. 5-Bromosalicylaldehyde was obtained from Aldrich (USA) and the corresponding 5-methyl, 5-chloro and 5,6-C_4H_4 derivatives were prepared in good yields by employing the Duff reaction.[24] Triphenylphosphine (Sisco Research Laboratories, India) was recrystallized twice from ethanol–water. Dimethylformamide used for the electrochemical and kinetics studies was dried by distillation *in vacuo* over P_2O_5 and then stored over Linde AW-500 molecular sieves. Dimethyl sulfoxide was distilled from CaH_2, degassed and stored under dinitrogen.

Preparation of the Ligands H_2L^1–H_2L^6.—The ligands were obtained *via* a Schiff-base condensation reaction between the appropriate aldehyde (0.02 mol) and *S*-methyldithiocarbazate (0.02 mol) in ethanol. Yields: 85–90% [Found: C, 47.9; H, 4.4; N, 12.4. $C_9H_{10}N_2OS_2(H_2L^1)$ requires C, 47.7; H, 4.4; N, 12.4. Found: C, 50.2; H, 5.0; N, 11.7. $C_{10}H_{12}N_2OS_2(H_2L^2)$ requires C, 50.0; H, 5.0; N, 11.6. Found: C, 41.4; H, 3.5; N, 10.8. $C_9H_9ClN_2OS_2(H_2L^3)$ requires C, 41.4; H, 3.5; N, 10.7. Found: C, 35.4; H, 3.3; N, 9.3. $C_9H_9BrN_2OS_2(H_2L^4)$ requires C, 35.4; H, 3.0; N, 9.2. Found: C, 40.0; H, 3.3; N, 15.6. $C_9H_9N_3O_3S_3(H_2L^5)$ requires C, 39.8; H, 3.3; N, 15.5. Found: C, 56.7; H, 4.4; N, 10.3. $C_{13}H_{12}N_2OS_2(H_2L^6)$ requires C, 56.5; H, 4.4; N, 10.1%].

Preparation of the Complexes $[MoO_2L]$ (L = L^1 **1a**, L^2 **1b**, L^3 **1c**, L^4 **1d**, L^5 **1e** or L^6 **1f**).—To a hot solution of the ligand (1 mmol) in ethanol or methanol (20 cm^3), was added a solution of $[MoO_2(acac)_2]$ (0.32 g, 1 mmol) in the same solvent (10 cm^3). The reaction mixture was gently refluxed for 30 min. It was then allowed to stand at 5 °C overnight whereupon the brown crystalline products formed were filtered off, washed with ethanol and dried *in vacuo*. Yield: 60–65%.

$[MoO_2L^1(D)]$ [D = *pyridine* (*py*) **1g**, *dmf* **1h** *or* Me_2SO **1i**] *and* $[MoO_2L(py)]$ (L = L^2 **1j**, L^3 **1k** *or* L^4 **1l**). These compounds were prepared by treating $[MoO_2L]$ with an excess of the monodentate donor ligands in ethanol. Yields: 60–65%.

$[MoO(L^1)]$ **2a**. A solution of $[MoO_2L^1]$ (1 mmol) was dissolved in either methanol, dichloromethane or acetonitrile (50 cm^3) by heating. Triphenylphosphine (0.4 g, 1.5 mol) was added as a solid to the solution with constant stirring. The reaction mixture was heated on a water-bath for 20 min producing a dark brown compound. The resulting precipitate was filtered off, and washed with ethanol. Yield: 85%.

[MoO(L)] (L = L^2 **2b**, L^3 **2c** *or* L^4 **2d**). Complexes, **2b**–**2d**, were prepared directly from $[MoO_2(acac)_2]$ by refluxing first with the respective ONS ligand and then with triphenylphosphine in methanol. Yields: 80%.

[MoOL(D)] (L = L^1, D = *dmf* **2e** *or py* **2f**; L = L^4, D = *dmf* **2g** *or py* **2h**). These compounds were prepared in the same manner as described for **2a**, using pyridine or dmf instead of methanol, acetonitrile or dichloromethane. Yields: ≈80%.

The analytical data for the isolated complexes are shown in Table 1.

Results and Discussion

(*a*) *Oxomolybdenum*(VI) *Complexes.*—Like H_2L',[16] the free ligands H_2L^1–H_2L^6 (see structures **A** and **B**) used in this work exhibit identical vibrational[25] spectra characterising their functionalities. After metal co-ordination the vibrational bands are identically modified as for the H_2L' complexes[16] indicating the attachment of H_2L ligands as L^{2-} obtained *via* the thiol form[26] **B**. The characteristic blue and red shifts[16] of the specific ligand functions[25,27] upon co-ordination, indicated that the MoO_2^{2+} group is bonded through the phenolic oxygen and azomethine nitrogen, besides the thiol sulfur. Moreover, comparison of the ^{1}H NMR spectra of H_2L^1–H_2L^5 with those of the complexes **1a**–**1e** reveals that the signals of (*i*) the phenolic protons, (*ii*) the azomethine protons[28] (Table 2) and (*iii*) the position of the –SMe proton resonance in all the ligands, occurring at *ca.* δ 2.72, undergo virtually identical shifting as observed for the $[MoO_2L']$ complexes,[16] supporting an ONS mode of co-ordination suggested from the IR data. Further endorsement comes from the appearance of new bands at 550–600, 415–440 and 340–345 cm^{-1} due to ν(Mo–O),[16] ν(Mo–N) and ν(Mo–S)[16] stretches, respectively, in **1a**–**1f**.

All the complexes **1a**–**1f** show a typical band at 805 cm^{-1} assignable to the Mo···O→Mo vibration,[17] besides a terminal ν(Mo=O) vibration at *ca.* 935 cm^{-1}, indicating the formation of polymeric complexes $[(MoO_2L)_n]$ containing . . . (O)Mo=O→Mo(O) . . . chains.[17,18] Hence, the structure of **1a**–**1f** can be represented as **C** where the ONS functionalities span the three meridional positions in a pseudo-octahedral geometry. Curiously, in the polymeric $[(MoO_2L')_n]$ complexes[16] there appear three other bands in the ν(Mo=O) vibrational region, besides the band at 805 cm^{-1} due to the bridging oxo group, whilst in the present complexes, **1a**–**1f**, only one such ν(Mo=O)

* Ligands L$^{1'}$–L$^{4'}$ are the –SCH_2Ph analogues of the –SMe ligands L^1–L^4.

Table 1 Analytical,[a] IR (cm^{-1})[b] and electronic spectral data[c] for the complexes

Complex	Analysis (%) C	H	N	Mo	ν(Mo=O)[d]	Selected D vibrations	ν(C–O)	λ_{max}/cm^{-1} (log ε/dm^3 mol^{-1} cm^{-1})
1a $[MoO_2L^1]$	30.7 (30.6)	2.2 (2.3)	8.0 (7.9)	27.2 (27.1)	930, 810[e]	—	1555m	23 696 (3.04)
1b $[MoO_2L^2]$	33.0 (32.8)	2.8 (2.7)	7.6 (7.6)	25.9 (26.2)	935, 810[e]	—	1560m	23 256 (3.10)
1c $[MoO_2L^3]$	28.2 (27.9)	1.9 (1.8)	7.0 (7.2)	24.4 (24.8)	938, 800[e]	—	1556m	23 866 (3.07)
1d $[MoO_2L^4]$	25.2 (25.1)	1.7 (1.6)	6.2 (6.5)	22.0 (22.2)	935, 800[e]	—	1555m	23 866 (3.07)
1e $[MoO_2L^5]$	27.3 (27.2)	1.9 (1.8)	10.4 (10.6)	23.8 (24.1)	920, 800[e]	—	1557m	24 760 (3.18)
1f $[MoO_2L^6]$	39.0 (38.8)	2.5 (2.5)	7.0 (6.9)	24.0 (23.8)	920, 820[e]	—	1558s	21 740 (3.10)
1g $[MoO_2L^1(py)]$[f]	38.8 (39.0)	3.1 (3.0)	9.8 (9.7)	22.4 (22.2)	920, 898	1455s, 1035m	1556s	23 256 (3.08)
1h $[MoO_2L^1(dmf)]$[f]	33.7 (33.9)	3.6 (3.5)	10.0 (9.9)	22.7 (22.5)	927, 900	1655s,[g] 685m[h]	1558m	23 474 (3.04)
1i $[MoO_2L^1(Me_2SO)]$[f]	30.9 (30.7)	3.2 (3.3)	6.7 (6.5)	22.5 (22.3)	920, 895	1015s[i]	1556m	23 640 (3.10)
1j $[MoO_2L^2(py)]$	40.8 (40.4)	3.4 (3.4)	9.5 (9.4)	20.9 (21.5)	928, 902	1450m, 1040m	1557s	23 410 (3.02)
1k $[MoO_2L^3(py)]$	36.4 (36.1)	2.6 (2.6)	8.8 (9.0)	20.2 (20.6)	930, 902	1450m, 1045m	1556m	23 310 (3.08)
1l $[MoO_2L^4(py)]$	33.1 (32.9)	2.5 (2.4)	8.0 (8.2)	18.9 (18.8)	925, 900	1450m, 1050m	1555 (sh)	23 310 (3.09)
2a $[MoO(L^1)]$	32.2 (32.1)	2.3 (2.4)	8.4 (8.3)	28.4 (28.5)	965	—	1554s	21 550 (3.43), 14 390 (3.00)
2b $[MoO(L^2)]$	34.7 (34.3)	2.9 (2.9)	7.8 (7.8)	27.1 (27.4)	970	—	1558m	21 550 (3.45), 14 285 (2.08)
2c $[MoO(L^3)]$	29.5 (29.2)	1.9 (1.9)	7.7 (7.6)	25.6 (25.9)	972	—	1558m	21 645 (3.44), 14 470 (2.05)
2d $[MoO(L^4)]$	26.3 (26.1)	1.7 (1.7)	6.8 (6.8)	23.0 (23.2)	970	—	1557m	21 645 (3.44), 14 325 (2.03)
2e $[MoOL^1(dmf)]$[j]	35.3 (35.2)	3.6 (3.7)	10.4 (10.2)	23.1 (23.4)	970	1655s,[g] 685m[h]	1556m	*k*
2f $[MoOL^2(py)]$	40.6 (40.5)	3.0 (3.1)	10.3 (10.1)	23.4 (23.1)	975	1455s, 1040m	1556m	21 275 (3.73), 14 535 (1.97)
2g $[MoOL^3(dmf)]$	29.7 (29.5)	3.0 (2.9)	8.7 (8.6)	19.2 (19.0)	962	1650s,[g] 680m[h]	1554m	*k*
2h $[MoOL^4(py)]$	34.2 (34.0)	2.4 (2.4)	8.6 (8.5)	19.1 (19.4)	960	1450m, 1010m	1556m	21 460 (3.73), 14 535 (1.97)

[a] Calculated values given in parentheses. [b] As KBr disc. [c] In dmf; intraligand transitions are not listed. [d] All the absorptions are very strong. [e] Strong and broad band. [f] Thermal analysis data (temperature range; see text). [g] Amide I band. [h] δ(NCO). [i] ν(SO). [j] Molecular weight in MeCN–dmf: 412 (409). [k] Same as **2a** and **2c**, respectively.

Table 2 Selected cyclic voltammetric,[a] proton NMR[b] and FT-IR[c] data for oxomolybdenum(VI) complexes

Complex	E_{pc}/V(n[d])	δ(CH=N)[e]	Δδ[f]	ν(Mo=O)/ cm^{-1}
1a	−0.86 (0.97)[g]	8.66	0.32	928.8, 904.2
1b	−0.90	8.61	0.30	933.3, 902.9
1c	−0.84	8.64	0.34	930.0, 905.4
1d	−0.83	8.66	0.36	929.0, 905.4
1e	−0.76	8.74	0.18	928.9, 909.0

[a] Solvent dmf, solute concentration ≈10^{-3} mol dm^{-3}, reference electrode SCE. [b] Proton NMR in $CDCl_3$–$(CD_3)_2SO$ (10:1) at room temperature. [c] In dmf solution. [d] $n = Q/Q'$ where Q' is the calculated coulomb count for a one-electron transfer and Q is the observed value after exhaustive electrolysis of 0.001 mol of solute. [e] Signal for the free ligand: H_2L^1, 8.34; H_2L^2, 8.31; H_2L^3, 8.30; H_2L^4, 8.30; H_2L^5, 8.56. [f] $\Delta\delta = (\delta_{complex} - \delta_{ligand})$. [g] Coulometry was carried out at −1.06 V.

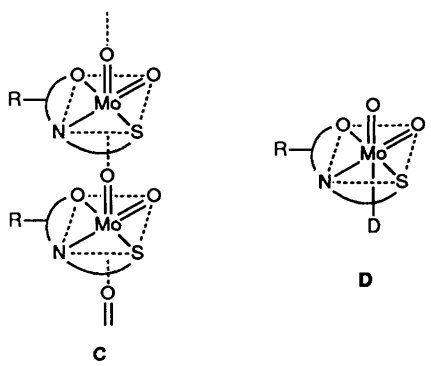

C

D

R = H, Me, Cl, Br, NO_2 or 5,6-C_4H_4

vibration appears. This indicates that MoO_2 complexes of L'^{2-} and L^{2-} ligands are not strictly isostructural. Also, when the complexes $[(MoO_2L)_n]$ **1a–1f** react with donor solvents D, such as pyridine (py), dmf or dimethyl sulfoxide (Me_2SO), to form monomeric complexes $[MoO_2L(D)]$ **1g–1l** the ν(Mo···O→Mo) vibration (*ca.* 805 cm^{-1}) disappears (Table 1), indicating a discrete monomeric structure **D** for the complexes. As expected,[16] each of the complexes **1a–1l** shows only one ligand-to-metal charge-transfer (l.m.c.t.) transition (see Table 1) in its electronic spectrum.

(*b*) *Oxomolybdenum*(IV) *Complexes*.—The oxomolybdenum(IV) species, [MoO(L)] (L = L^1–L^4, **2a–2d**) or [MoOL(D)] (L = L^1, D = dmf **2e** or py **2f**; L = L^4, D = dmf **2g** or py **2h**) are formed when the appropriate $[MoO_2L]$ complex reacts with PPh_3 in CH_2Cl_2, MeOH or MeCN or in the respective donor solvents (py or dmf), whereby the MoO_2^{2+} unit transfers one oxygen atom to PPh_3 converting it to $OPPh_3$. As such, **2a–2d** are polymeric[16,29] but show only one ν(Mo=O) vibration (Table 1) eliminating polymerisation *via* oxo bridging. Polymerisation involving phenoxide oxygen as bridging ligand is also not supported[16] by IR data (Table 1). Complexes **2a–2h** are diamagnetic and non-electrolytes in dmf. The donor-co-ordinated monomers, **2e–2h**, also show only a single ν(Mo=O) vibration (Table 1). Molecular weight data on **2f** (Table 1), further suggests that the species are monomeric and hence five-co-ordinate. This idea is nicely supported by thermoanalytical data. Mass-loss values calculated from the thermogravimetric analysis (TGA) curves of complexes **2e** and **2f** (Fig. 1) correspond to the loss of one dmf (**2e**) or py (**2f**). Interestingly, the differential thermal analysis (DTA) curves (Fig. 1) show that after the endothermic loss of the donor ligand, another exotherm appears at 180 (**2e**) or 200 °C (**2f**), which is not accompanied by any mass loss in the TGA curve. This can be attributed to phase transitions arising from a structural change in **2e** and **2f**, and by inference, also of **2g** and **2h**, from discrete five-co-ordinate species to polymeric entities. Assuming meridional disposition of the ONS ligand, as in the dioxomolybdenum(VI) complexes, a square-pyramidal geometry with a vacant co-ordination site *trans* to the Mo=O bond is a reasonable likelihood for the structures of **2e–2h**.

The electronic spectra of the [MoO(L)] complexes **2a–2d** in degassed dmf solution show two bands and are essentially the same as those of the dmf adducts (**2e** and **2g**) (Table 1). The bands appear at ≈462 and ≈690 nm (Table 1), very much as found for the H_2L' complexes.[16]

(*c*) *Electrochemistry*.—The cyclic voltammetry of the isolated dioxomolybdenum(VI) and oxomolybdenum(IV) complexes has

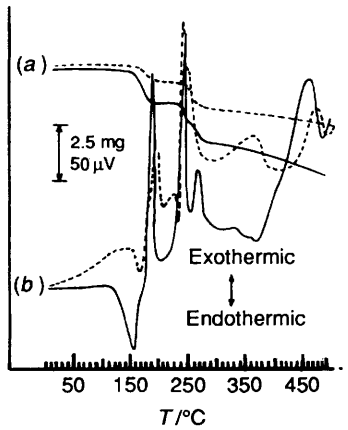

Fig. 1 TGA (*a*) and DTA (*b*) curves of [MoOL^1(dmf)] (——) and [MoOL^1(py)] (– – –)

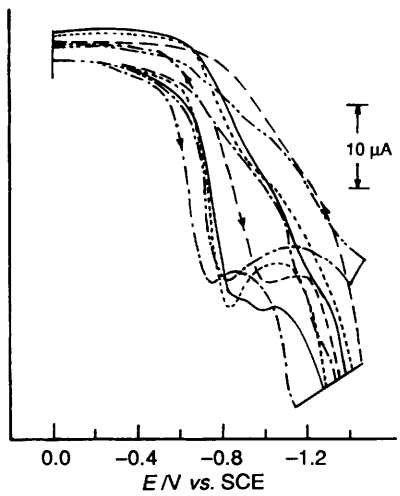

Fig. 2 Cyclic voltammograms for $\approx 10^{-3}$ mol dm^{-3} solutions of the [MoO_2L] complexes in dmf (scan rate 50 mV s^{-1}): R = H (——), Me (– – –), Cl (· · · ·), Br (— · · —) or NO_2 (— · —)

been studied using a platinum working electrode and NEt_4ClO_4 as supporting electrolyte in dmf solvent. Complexes **1a**–**1e** (Fig. 2) exhibit irreversible single-electron (exhaustive coulometry) reduction waves in their cyclic voltammograms at the potentials given in Table 2. No detectable oxidation wave was seen during the reverse anodic scans. This type of behaviour was also noted earlier for other dioxomolybdenum(VI) complexes.[6,16] The reduction potentials (E_{pc}) are sensitive to the nature of the 5-R substituents on the salicyl phenyl ring. As the substituents become more electron withdrawing (Me < H < Cl < Br < NO_2) the shift of E_{pc} of the $Mo^{VI} \rightarrow Mo^{V}$ couple becomes more anodic indicating easier reducibility of the respective molybdenum(VI) centres.

The cyclic voltammograms of the [MoOL^1(dmf)] complexes in dmf–NEt_4ClO_4 (0.1 mol dm^{-3}) exhibit an irreversible oxidative response at +0.15 V (*vs.* SCE) showing only a feeble reductive response in the reverse sweep at +0.05 V. On the negative side of the SCE, a cathodic scan shows a reduction wave at −0.97 V (*vs.* SCE) and the reverse sweep does not show any anodic counterpart, analogous to the H_2L' complexes.[16] The corresponding H_2L complexes with L^1–L^6 are unstable under the cyclic voltammetric experimental conditions. However, in the Mo^{IV}–H_2L' complexes, the values of E_{pa} move in the cathodic direction as indicated by the order R = Me < H < Cl ≈ Br (Table 3), parallelling the electronic effect transmitted by the substituents. Similarly, values of E_{pc} also shift in the anodic direction following the substituent order as indicated above.[6b]

Table 3 Comparison of cyclic voltammetric data[a] for molybdenum(IV) complexes[b]

Complex	E_{pc}/V	E_{pa}/V
[Mo(L^1)]	−0.97	+0.15
[MoO($L^{1'}$)][c,d]	−0.94	+0.42
[MoO($L^{2'}$)][d]	−0.98	+0.40
[MoO($L^{3'}$)][d]	−0.82	+0.45
[MoO($L^{4'}$)][d]	−0.83	+0.46

[a] Solvent dmf. [b] Ligands $L^{1'}$–$L^{4'}$ correspond to L^1–L^4 but with X = CH_2Ph instead of Me. [c] Data from ref. 16. [d] For **1a**–**1d** see Experimental section.

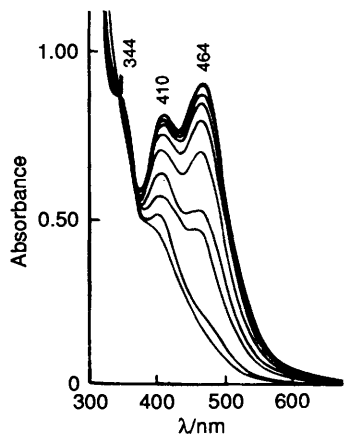

Fig. 3 Spectral changes in the reaction of [MoO_2L^1] (2 × 10^{-4} mol dm^{-3}) and PPh_3 (6 × 10^{-4} mol dm^{-3}) in CH_2Cl_2 solution at 25 °C

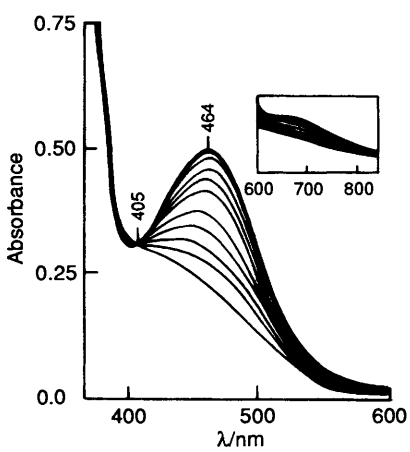

Fig. 4 Spectral changes in the reaction of [MoO_2L^1] (2 × 10^{-4} mol dm^{-3})

(*d*) *Kinetics.*—(*i*) *Oxo transfer from* Mo^{VI} *to substrate.* All the molybdenum(VI) complexes undergo oxygen-atom transfer reactions to the substrate, PPh_3, as shown in equations (2) and (3) forming [Mo^{IV}O(L)] or [Mo^{IV}OL(D)] as the products.

$$[MoO_2L^1] + PPh_3 \xrightarrow[k_2]{CH_2Cl_2} [MoO(L^1)] + OPPh_3 \quad (2)$$

$$[MoO_2L(dmf)]\ (L = L^1\text{–}L^4) + PPh_3 \xrightarrow[k_3]{dmf} [MoOL(dmf)] + OPPh_3 \quad (3)$$

These reactions (PPh_3 in excess) have been examined spectrophotometrically, as shown in Figs. 3 and 4. Plots of $\ln(A_\infty - A_t)$ against time (t) are linear (see Experimental

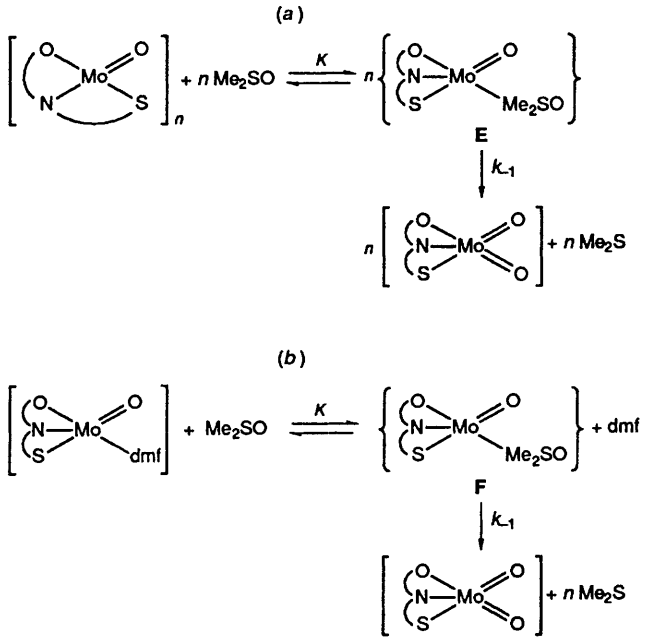

Scheme 1 (*a*) In CH_2Cl_2. (*b*) In dmf

Table 4 Kinetic data for oxo-transfer reactions of molybdenum-(VI) and -(IV) complexes

Complex	Substrate	Solvent	T/°C	10^3 × Rate constant[a]
1a	PPh_3	CH_2Cl_2	25	(5.60 ± 0.36) × 10^3 (k_2)
	PPh_3	dmf	30	14.87 ± 0.24 (k_3)
1b	PPh_3	dmf	30	12.62 ± 0.20 (k_3)
1c	PPh_3	dmf	30	18.08 ± 0.32 (k_3)
1d	PPh_3	dmf	30	18.59 ± 0.87 (k_3)
2a	Me_2SO	CH_2Cl_2	20	2.58 ± 0.11[b] (k_{-1})
2e	Me_2SO	dmf	20	6.15 ± 0.14[c] (k_{-1})

[a] k_2/dm^3 mol^{-1} s^{-1}, k_3/dm^3 mol^{-1} s^{-1}, k_{-1}/s^{-1}. [b] K = 16.5. [c] K = 79.0.

section) showing that the reaction is first-order in molybdenum complex. The dependence of k_{obs} on [PPh_3] is linear with a nearly zero intercept. As for other oxygen atom-transfer reactions from molybdenum(VI) complexes to PPh_3, the reactions follow the rate law, $-d[MoO_2L^1]/dt = k_2[MoO_2L^1][PPh_3]$ in CH_2Cl_2 or $-d[MoO_2L(dmf)]/dt = k_3[MoO_2L(dmf)][PPh_3]$ (L = L^1–L^4) in dmf. The oxo transfer is more facile for **1a**, studied in CH_2Cl_2 solvent in which the polymeric structure is retained, in comparison to that of **1h** (Table 4). This is due to the fact that compared to the terminal MoO_2 oxygens in the discrete mononuclear complexes, the Mo···O→Mo oxygen present in the oligomers is more labile and hence reacts faster with the substrate, leading to a higher rate constant value. This phenomenon in oxo-transfer reactions is reported here for the first time.

(*ii*) *Oxygen-atom transfer from substrate.* In order to assess the oxo-transfer behaviour of [$Mo^{IV}O$(ONS)] in CH_2Cl_2 and in dmf, kinetic studies were carried out under pseudo-first-order conditions using a concentration variation of Me_2SO (50–1000 molar excess). The oxygen-atom transfer from substrate to the $Mo^{IV}O$ core had previously been investigated in dmf for an NS_2 ligand.[20a] The present study has focussed attention on the modification of the reactivity of the complex molecule with a variation of solvents (donor *vs.* non-donor). Complexes [MoO(ONS)] and [MoO(ONS)(dmf)] react with Me_2SO in two steps (Scheme 1) to yield [MoO_2(ONS)] and Me_2S.

Spectrophotometric examination of the above reactions shows a clean isosbestic point at 358 nm (Fig. 5) in CH_2Cl_2 and at 382 nm (Fig. 6) in dmf. The final spectra are identical to

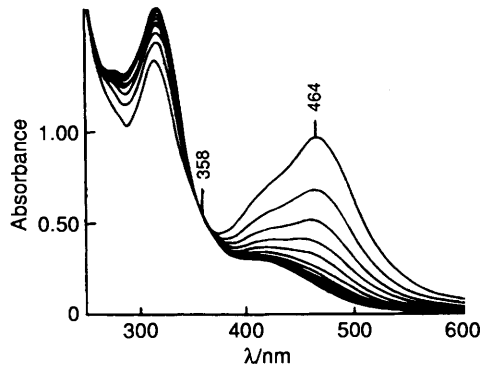

Fig. 5 Spectral changes in the reaction of [$MoO(L^1)$] (2 × 10^{-4} mol dm^{-3}) and Me_2SO (1.4 × 10^{-2} mol dm^{-3}) in CH_2Cl_2 solution at 20 °C

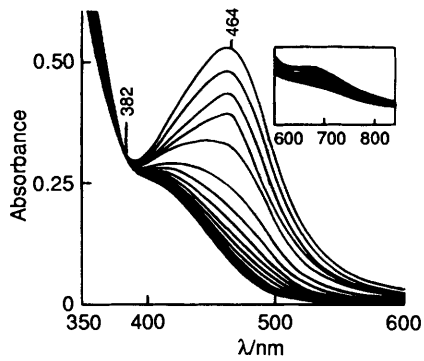

Fig. 6 Spectral changes in the reaction of [$MoOL^1$(dmf)] (2 × 10^{-4} mol dm^{-3}) and Me_2SO (2.8 × 10^{-2} mol dm^{-3}) in dmf solution at 20 °C

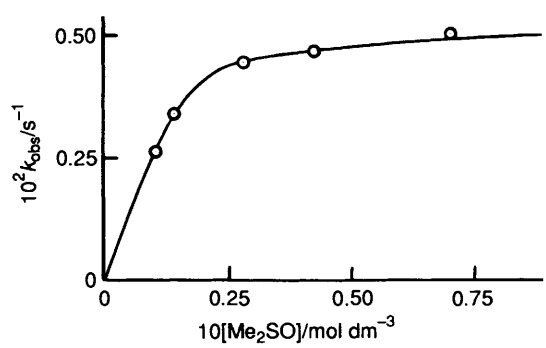

Fig. 7 Dependence of the rate of reaction of [$MoOL^1$(dmf)] in dmf solution at 20 °C with concentration of Me_2SO

those of the isolated [$MoO_2L(Me_2SO)$] complexes. The plots of $\ln(A_t - A_\infty)$ against t are linear up to four half-lives of the reactions, indicating a first-order dependence of rate on the molybdenum(IV) complexes. Again, a plot of the observed rates against [Me_2SO] shows that at sufficiently high concentrations the rates (k_{obs}), become virtually independent of [Me_2SO], *i.e.*, substrate saturation kinetics is obtained (Fig. 7).

As is apparent from Scheme 1, in dmf solution, an equilibrium exists between the dmf- and sulfoxide-ligated molybdenum(IV) complexes. On the other hand, in CH_2Cl_2 medium, an equilibrium exists between [{MoO(L)}$_n$] and n[MoOL(Me_2SO)]. As for other oxygen-atom transfer reactions from Me_2SO to molybdenum(IV) complexes in dmf, the rate law[20a] is given by equation (4) (Y = dmf + Me_2SO).

$$\frac{d[MoOL(Y)]}{dt} = -k_{-1}[MoOL(Me_2SO)] = -k_{-1}\left\{\frac{K[Me_2SO]}{K[Me_2SO] + [dmf]}\right\}[MoOL(Y)] \quad (4)$$

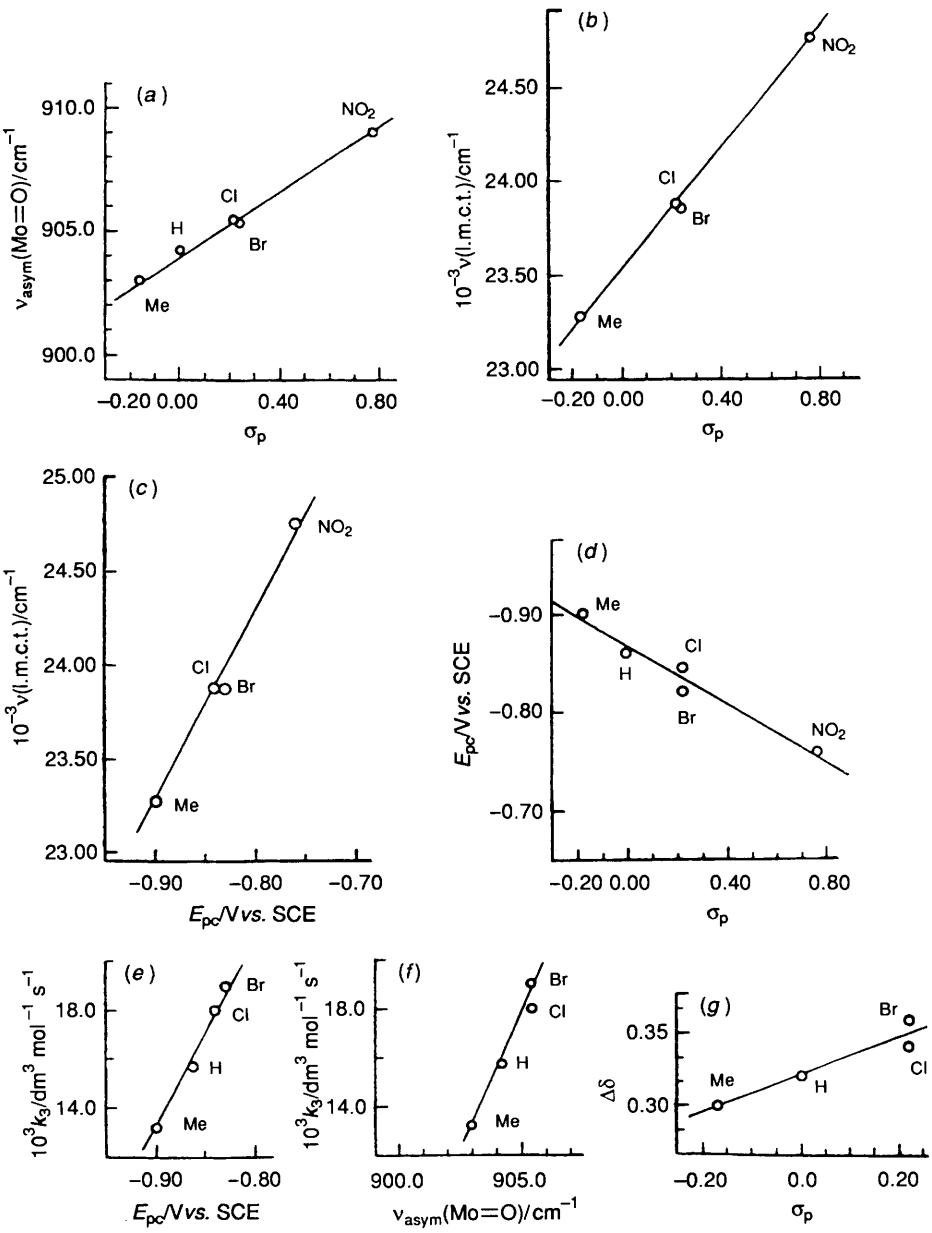

Fig. 8 Plot of (*a*) ν_{asym}(Mo=O) *vs.* Hammett σ_p; (*b*) l.m.c.t. *vs.* σ_p; (*c*) l.m.c.t. *vs.* E_{pc}; (*d*) E_{pc} *vs.* σ_p; (*e*) k_3 *vs.* E_{pc}; (*f*) k_3 *vs.* ν_{asym}(Mo=O); (*g*) Δδ *vs.* σ_p [note that the abscissa is not extended up to $\sigma_p(NO_2)$ (see text)]; for $[MoO_2L(dmf)]$ [L = L^1 (R = H), L^2 (R = Me), L^3 (R = Cl), L^4 (R = Br) or L^5 (R = NO_2)]

In CH_2Cl_2 the reaction follows a simpler rate law[30] given by equation (5).

$$\frac{d[MoOL(Me_2SO)]}{dt} = -k_{-1}[MoO(L)][Me_2SO] = \frac{-k_{-1}K[Me_2SO]}{1 + K[Me_2SO]} \quad (5)$$

Parameter k_{-1} denotes the rate constant accompanying the intramolecular oxo transfer from co-ordinated substrate, Me_2SO, to the [MoO(L)] moiety as shown in Scheme 1, and values of K are the respective equilibrium constants of the reactions. The values of k_{-1} and K were evaluated from plots of $1/k_{obs}$ *vs.* $1/[Me_2SO]$, and the same values are obtained from the reciprocals of the intercepts and slopes,[20a] respectively (Table 4) of the straight lines thus obtained. The equilibrium constants for **2a** and **2e**, are two orders of magnitude lower than that for the reaction of Me_2SO with an $[MoO(NS_2)(dmf)]$ complex,[20a] but the rates of the oxo transfer are almost the same. Thus, the activated species in our ONS ligated complex is thermodynamically less stable than that of the NS_2 ligated system.[20a] Again, comparing the K values of the polymeric and monomeric species described here, it is found that the values are only slightly smaller for **E** than for **F**. This may be apparent from Scheme 1, which implies that **E** is derived by the breaking of polymers to monomers assisted by Me_2SO co-ordination, while **F** is generated *via* a nucleophilic substitution reaction.

(*e*) *Influence of Ligand Substituents on the Structural and Electronic Aspects of the Complexes.*—The unco-ordinated S–Me group present in the H_2L ligands renders the molybdenum centre in the MoO_2 complexes too electron rich to exhibit discriminatory properties in forming both monomeric or polymeric complexes for the range of 5-R substituents [H (0.00),* Me (−0.17), Cl, Br (+0.22), NO_2 (+0.77)] or 5,6-C_4H_4 studied here. As a result, only the polymers, $[(MoO_2L)_n]$ **1a**–**1f**,

* Figures in parentheses indicate the respective Hammett σ_p parameter.

have been obtained. This electron richness makes $[MoO_2L]$ species less easily reducible than the corresponding complexes $[MoO_2L']$ (compare Table 2 with Table 3 of ref. 16). Interestingly, this behaviour is also reflected in the oxomolybdenum(IV) complexes. The E_{pa} value for the Mo^{IV}–Mo^{V} couple for $[MoOL^1(dmf)]$ (Table 3) is found to be more cathodic than that of the corresponding $[MoOL'(dmf)]$ (R = H) species (Table 3). Similarly, the E_{pc} value for the Mo^{IV}–Mo^{III} couple in the oxomolybdenum(IV) also becomes more cathodic for X = Me(L) compared to X = CH_2Ph (L') (Table 3).

However, despite the levelling effect (coarse tuning) imposed on the R substituents by the electron-donating methyl substituent towards the position of the monomer–polymer equilibrium, the nature of the R substituents still controls (by fine tuning) various spectroscopic, electrochemical and reactivity parameters of the respective polymers or $[MoO_2L(D)]$ complexes derived from these. These parameters include the position of the ν(Mo···O→Mo) and ν(Mo=O) vibrations, the band position of the $S_{p\pi}$→$Mo_{d\pi}$ l.m.c.t. transition, the Mo^{VI}–Mo^{V} reduction potential for the MoO_2 complexes, the oxidation (Mo^{IV}–Mo^{V}) and reduction (Mo^{IV}–Mo^{III}) potentials of the [MoO(L)] complexes, the rate constant of the oxo-transfer reaction represented by the forward reaction in equation (1) and the position of azomethine proton resonances in appropriate complexes. Regarding the position of the ν(Mo···O→Mo) vibration, the gross substituent dependence is $NO_2 \approx Br \approx Cl < H \approx Me < 5,6\text{-}C_4H_4$ (Table 1) indicating that electron-withdrawing substituents destabilize the oxygen bridges. Interestingly, the ν_{asym}(Mo=O) vibration (Table 2), and the energy (in cm^{-1}) of the l.m.c.t. electronic transition, of $[MoO_2L(dmf)]$ (L = L^1–L^5) (Table 1) in dmf solution, show a linear correlation[9] with the Hammett σ_p values of the R substituents (Fig. 8). Similarly for the $[MoO_2L^1(D)]$ (D = py **1g**, dmf **1h** or Me_2SO **1i**) complexes, the ν_{asym}(Mo=O) vibration in the solid state increases in the order D = Me_2SO < py < dmf. The temperature loss of donor molecules D (TGA data) for the above complexes in the solid state also decreases in the same order indicating that strong donor binding to molybdenum reduces $O_{p\pi}$→$Mo_{d\pi}$ overlap in the MoO_2^{2+} moiety.

An investigation into the redox chemistry of the $[MoO_2L]$ complexes suggests that a linear dependence exists between values of E_{pc} (Table 2) and the Hammett σ_p parameter of the R substituents[6b] of the respective ligands, and also between E_{pc} and positions of the l.m.c.t. transitions (Fig. 8). This demonstrates the sensitivity of the molybdenum electron density (and hence the optical electronegativity of the metal) on the Hammett σ_p parameter of the R substituent.

Also, the extent of the downfield shift (Δδ) of the azomethine proton signal of H_2L upon complexation is less in the present complexes (X = Me) than the corresponding values observed in complexes with L' (X = CH_2Ph).[16] For the present series of complexes Δδ varies linearly with the Hammett σ_p values of the R substituent (except for R = NO_2, see Fig. 8).

Finally, the observed oxo-transfer rate constant (k_3) from $[MoO_2L(dmf)]$ to PPh_3 shows a linear relationship with the values of E_{pc} for the Mo^{VI}–Mo^{V} couples (Fig. 8). This indicates that the electronic effects that cause systematic changes in E_{pc} values also modify the electrophilicity of the oxide ligands which is manifested in their acceptor properties towards phosphorus donors.

All these correlations indicate the prominence of ligand control (by variation of R) towards metal reactivity in these systems.

Conclusion

The nature of the neighbouring group SX attached to a >C–SH functionality imparts a profound electronic effect at the metal centre depending on the nature of X. When X is an ambivalent substituent, *e.g.* CH_2Ph, the mono- or oligonuclearity of the resulting ONS donor complex depends on the nature of the R substituents attached to the salicyl phenyl groups. However when X is an electron-repelling group such as Me, the complex $[MoO_2(L)]$ is always an oligomer irrespective of the nature of the R substituents. For the oligomeric complexes $[(MoO_2L)_n]$, or in the donor-co-ordinated monomers $[MoO_2L(D)]$ obtained from the oligomers, the R substituent almost quantitatively controls various spectroscopic, electrochemical and reactivity parameters of the complexes. For the MoO_2 complexes the rate of oxo transfer to PPh_3 substrate is much higher when the oxygen atom involved occurs as a bridge between two molybdenum atoms, Mo···O→Mo, $\{[(MoO_2L)_n]\}$ rather than as a terminal oxygen of the MoO_2^{2+} group $\{[MoO_2L(D)]\}$.

Acknowledgements

Financial assistance from the Indian Council for Cultural Relations, and the Council of Scientific and Industrial Research, New Delhi, is gratefully acknowledged. S. B. thanks the Indian Council for Cultural Relations, Foreign Students Division, New Delhi, for a research fellowship. We also thank Professor A. Chakravorty (Indian Association for the Cultivation of Science, Calcutta) for electrochemistry and Professor A. K. Barua of the same institute for FT-IR facilities. The authors extend their thanks to Professor P. Banerjee of the above institute for helping with the kinetic studies. We thank the Alexander von Humboldt Foundation, Germany, for donating the IR spectrophotometer used in this work.

References

1 R. H. Holm, *Chem. Rev.*, 1987, **87**, 1401 and refs. therein.
2 R. C. Bray, *The Enzymes*, ed. P. D. Boyer, Academic Press, New York, 1975, 3rd edn., vol. 12, part B, ch. 6.
3 M. P. Coughlan (Editor), *Molybdenum and Molybdenum Containing Enzymes*, Pergamon, New York, 1980.
4 W. E. Newton and S. Otsuka (Editors), *Molybdenum Chemistry of Biological Significance*, Plenum, New York, 1980.
5 A. del-Campillo-Campbell and A. Campbell, *J. Bacteriol.*, 1982, **149**, 469.
6 (*a*) J. Topich and J. T. Lyon, III, *Polyhedron*, 1984, **3**, 55, 61; (*b*) J. Topich, *Inorg. Chem.*, 1981, **20**, 3704; (*c*) J. Topich and J. T. Lyon, III, *Inorg. Chem.*, 1984, **23**, 3202.
7 O. A. Rajan and A. Chakravorty, *Inorg. Chim. Acta*, 1979, **37**, L503.
8 A. Nakamura, M. Nakayama, K. Sugihashi and S. Otsuka, *Inorg. Chem.*, 1979, **18**, 394.
9 J. Topich and J. O. Bachert, III, *Inorg. Chem.*, 1992, **31**, 511.
10 J. M. Berg and R. H. Holm, *J. Am. Chem. Soc.*, 1985, **107**, 917.
11 S. A. Roberts, C. G. Young, C. A. Kipke, W. E. Cleland, jun., K. Yamanouchi, M. D. Carducci and J. H. Enemark, *Inorg. Chem.*, 1990, **29**, 3650.
12 S. P. Cramer, H. B. Gray and K. V. Rajagopalan, *J. Am. Chem. Soc.*, 1979, **101**, 2772.
13 J. M. Berg, K. O. Hodgson, S. P. Cramer, J. L. Corbin, A. Elsberry, N. Pariyadath and E. I. Stiefel, *J. Am. Chem. Soc.*, 1979, **101**, 2774.
14 S. P. Cramer, R. Wahl and K. V. Rajagopalan, *J. Am. Chem. Soc.*, 1981, **103**, 7721.
15 T. D. Tullius, D. M. Jr. Kurtz, S. D. Conradson and K. O. Hodgson, *J. Am. Chem. Soc.*, 1979, **101**, 2776.
16 S. Bhattacharjee and R. G. Bhattacharyya, *J. Chem. Soc., Dalton Trans.*, 1992, 1357.
17 O. A. Rajan and A. Chakravorty, *Inorg. Chem.*, 1981, **20**, 660.
18 J. M. Berg and R. H. Holm, *Inorg. Chem.*, 1983, **22**, 1768.
19 C. T. Kan, *J. Chem. Soc., Dalton Trans.*, 1982, 2309.
20 (*a*) J. M. Berg and R. H. Holm, *J. Am. Chem. Soc.*, 1985, **107**, 925; (*b*) M. S. Reynolds, J. M. Berg and R. H. Holm, *Inorg. Chem.*, 1984, **23**, 3057; (*c*) J. Topich and J. T. Lyon, III, *Inorg. Chim. Acta*, 1983, **80**, L41.
21 A. I. Vogel, *A Text Book of Quantitative Inorganic Analysis*, The English Language Book Society and Longmans, London, 1968.
22 M. A. Ali, S. E. Livingstone and D. J. Phillips, *Inorg. Chim. Acta*, 1973, **7**, 179.
23 C. C. Hach, L. M. Liggett and H. Diehl, *Chem. Abstr.*, 1948, **42**, 1240h.
24 J. C. Duff, *J. Chem. Soc.*, 1941, 547.

25 M. A. Ali and R. Bose, *J. Inorg. Nucl. Chem.*, 1977, **39**, 265.
26 M. A. Ali, D. A. Chowdhury-I and M. Nazimuddin, *Polyhedron*, 1984, **3**, 595.
27 J. E. Kovacic, *Spectrochim. Acta, Part A*, 1967, **23**, 183.
28 A. Saxena, J. P. Tandon, K. C. Molloy and J. J. Zuckerman, *Inorg. Chim. Acta*, 1982, **63**, 71.
29 E. I. Stiefel, *Prog. Inorg. Chem.*, 1977, **22**, 1.
30 R. G. Wilkins, *The Study of Kinetics and Mechanism of Reactions of Transition Metal Complexes*, Allyn and Bacon, Boston, 1974.

Received 5th August 1992; *Paper* 2/04236C